Understanding anthracycline action: molecular insights to improve cancer therapy

Gelder, M.A. van

CHAPTER 3

Genome-Wide CRISPR-Screening Identifies p53 as Regulator of Cancer Cell Sensitivity to the Histone Evicting Anthracycline Aclarubicin

Sabina Y. van der Zanden[1], Merle A. van Gelder[1], Amina Teunissen[1], Aart G. Jochemsen[1], Ruud H.M. Wijdeven[1,2] & Jacques Neefjes[1]

[1] Department of Cell and Chemical Biology, ONCODE institute, Leiden University Medical Center, 2333 ZC Leiden, The Netherlands.

[2] Alzheimer Center Amsterdam, department of Neurology, Amsterdam Neuroscience Amsterdam, University Medical Center Amsterdam, The Netherlands.

Submitted to Cell Death and Disease

Abstract

The anthracycline family, with its prime member doxorubicin, is one of the cornerstones in cancer chemotherapy and acts by poisoning topoisomerase II, resulting in DNA double stranded breaks. One of its members, aclarubicin, is considered a distinct member of the family due to its inability to inflict DNA double strand breaks. Despite this, aclarubicin is an effective anti-cancer drug by evicting histones resulting in chromatin damage. How aclarubicin-induced chromatin damage induces cell death remains largely unknown. Here, we performed a genome-wide CRISPR screen to identify factors regulating sensitivity of cells to aclarubicin and identified p53 as a critical factor for cellular sensitivity. Even though aclarubicin does not induce DNA breaks, treatment resulted in a swift initiation of the p53 DNA damage pathway by stabilization and activation of p53, and subsequent induction of apoptosis. Furthermore, response to aclarubicin treatment could fairly well be predicted in cell lines solely based on p53-status. These data suggest that p53 can be activated for apoptosis induction by at least two different pathways, DNA- and chromatin damage. Together, these data suggest p53 could be an important factor to stratify patients for the treatment with Aclarubicin.

Introduction

Aclarubicin belongs to the family of anthracycline drugs, which are among the most widely used anti-cancer drugs. Including other members like doxorubicin, epirubicin, daunorubicin and idarubicin, these drugs are used to treat a wide spectrum of tumors.[1,2] The classical mechanism of action of anthracyclines is poisoning of topoisomerase II, via intercalation of the compound into the DNA and formation of topoisomerase II-DNA complexes.[3,4] These formed adducts result in enzyme-mediated DNA double strand breaks, inducing activation of p53 and DNA damage response pathways for cell cycle arrest and/or cell death.[5] Aclarubicin, on the other hand, inhibits topoisomerase at a different step in the catalytic cycle, preventing enzyme binding to the DNA.[3,4] As a consequence, treatment with aclarubicin does not lead to induction of DNA breaks.[6–8] The anthracyclines differ from other topoisomerase II poisons, such as the podophyllotoxin etoposide, as that they have a second mechanism of action. When the anthraquinone moiety of anthracyclines intercalates into the DNA double helix, the sugar moiety emanates into the DNA minor groove and competes with histones for space, causing destabilization of nucleosomes and eviction of histones.[4,6,9] This activity has multiple consequences, including attenuated DNA damage responses, altered transcriptomics and deregulation of the epigenome at defined regions of the genome, collectively referred to as chromatin damage.[6,8] Evaluation of this activity amongst various anthracycline variants has shown that chromatin damage is essential to the effectivity of this class of anti-cancer drugs.[7,10,11] This is illustrated by the anthracycline amrubicin and the topoisomerase inhibitor etoposide, which are abstained from chromatin damage activity and considerably less effective.[7] Furthermore, the combination of DNA- and chromatin damage (as is the case for doxorubicin, epirubicin, daunorubicin and idarubicin) has been shown to conspire to cause a number of severe side effects [8], including dose-dependent cardiotoxicity, therapy-related malignancies and gonadotoxicity.[12,13] On the contrary, variants deficient for DNA damage activity, such as aclarubicin, lack the severe side effects displayed by the other family members.[7]

Although aclarubicin is an effective anti-cancer drug used for the treatment of AML patients[14], the mechanism by which chromatin damage leads to cell death is not fully understood. Therefore, we performed a genome-wide CRISPR knockout screen to identify regulators of aclarubicin sensitivity, yielding p53 as the most prominent hit. Indeed, p53 depletion decreased sensitivity to aclarubicin, and mutational status of p53 could be used as a proxy for sensitivity of cells to aclarubicin. Mechanistically, aclarubicin treatment leads to DNA-binding, phosphorylation and stabilization of p53, resulting in induction of apoptosis even in the absence of DNA breaks. Thus, chromatin damage induced by aclarubicin can be sensed by p53 and translated into a cellular response also observed in a DNA damage response leading to the induction of cell death. Together, this uncovers a second mechanism of induction of p53-mediated apoptosis by anthracycline cancer drugs.

Results

CRISPR-screening identifies p53 as regulator of aclarubicin sensitivity

Doxorubicin is a widely used chemotherapeutic that by intercalation into the DNA traps the enzyme topoisomerase II, forming a drug-DNA-enzyme adduct resulting in the formation of DNA double strand breaks.[3] Furthermore, intercalation into the DNA leads to the induces chromatin damage via eviction of histones (Fig. 1A).[6,15] Unlike doxorubicin, this dual action mechanism is not observed for all clinical relevant anthracyclines drugs, where amrubicin only induces DNA double strand breaks (Fig. 1A and S1A) and aclarubicin has only histone eviction activity (Fig. 1A and S1B). However, how chromatin damage activity induces cell death remains unclear. To identify proteins contributing to aclarubicin induced cell death following chromatin damage, we performed a genome-wide CRISPR knockout screen. MelJuSo melanoma cells were used as model cell line, since these are fairly sensitive to aclarubicin (IC_{50} of about 100nM) and take up the drug efficiently.[6,7] Cells were transduced with the Brunello genome-wide CRISPR library (4 gRNAs per gene) and treated five days later with aclarubicin for nine days at a concentration of 100nM (Fig. 1B). After this, surviving cells were harvested, genomic DNA was isolated, sequenced and compared to the untreated control. Hit calling was based on statistical significance in both biological replicates using RSA analysis, as well as an absolute fold enrichment of > 2.5 for at least 2 gRNAs per gene. This yielded two prominent hits: apoptotic TRAIL receptor DR4 (encoded by TNFRSF10A) and tumor suppressor p53 (TP53) (Fig. 1C and S1C). Lower hits included Caspase-8 and FADD, the two signaling adaptors for DR4, as well as the transcriptional regulators DR1 and CBFB. However, the fold enrichments for these hits were low, suggesting only a minor contribution of these genes to aclarubicin sensitivity. Overall, these results suggest a role for p53 and apoptotic signaling in aclarubicin sensitivity.

To validate the involvement of p53 in aclarubicin sensitivity, we transduced MelJuSo cells with the top two gRNAs from the screen, creating two different pools of p53-deficient cells. One of these yielded a robust depletion of p53, whereas gRNA #2 (which targets the domain of TP53 involved in DNA binding) lead to mutated p53 protein (Fig. 1D and S1D). Importantly, both cell lines were completely insensitive to treatment with the MDM2-inhibitor RG7112 that stabilizes p53, validating the generation of two functional TP53-knockout cell lines (Fig. 1E). These p53-knockout MelJuSo cells were more resistant to aclarubicin following continuous 72hrs exposure and short pulse treatment (Fig. 1F and S1E), as well as in long-term colony forming assays (Fig. 1G and H). Thus, our CRISPR-screen identified a role for p53 in sensitivity of cells to aclarubicin.

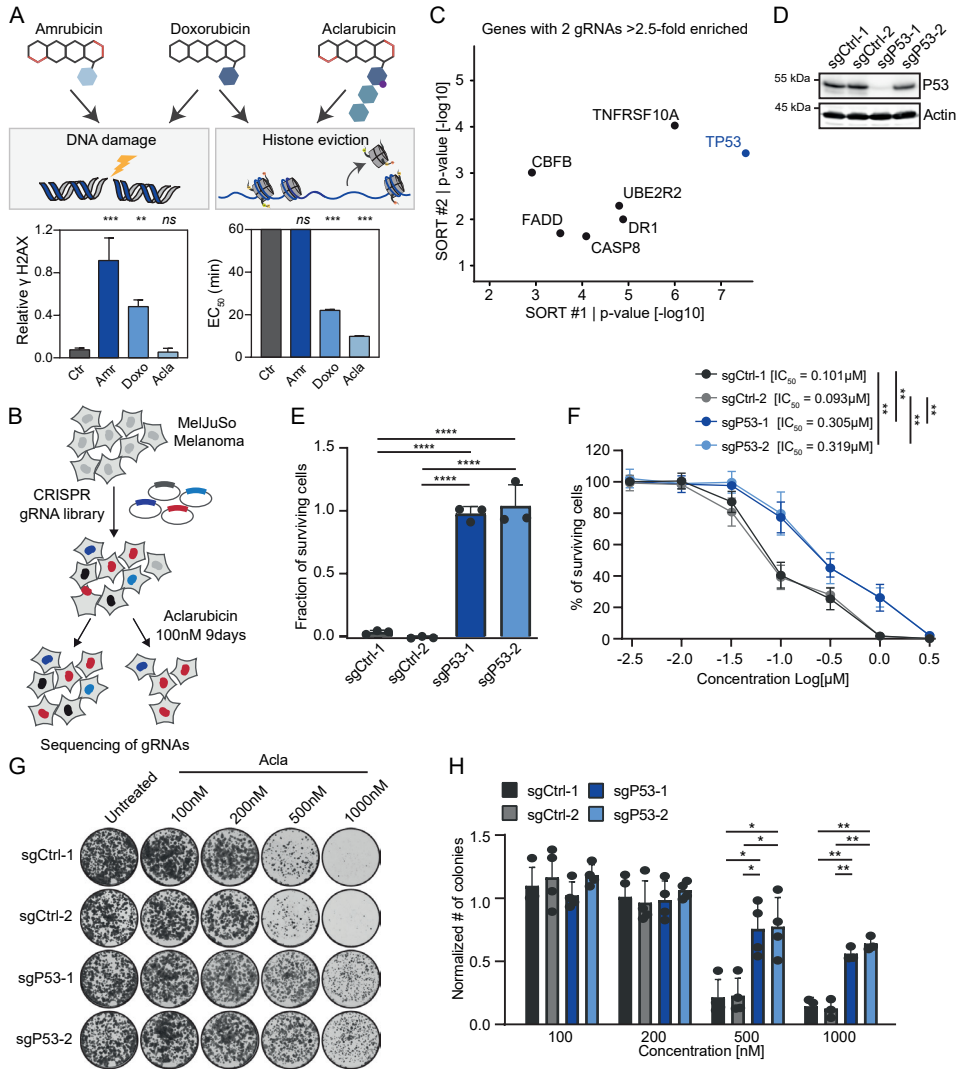

Fig. 1 genome-wide CRISPR screening identifies p53 as a regulator of sensitivity to Aclarubicin. **A** Top panel: Schematic overview of the DNA damage (via targeting topoisomerase II) and chromatin damage (via eviction of histones) activity of amrubicin, doxorubicin and aclarubicin. Bottom panel: DNA double strand breaks induced by these three anthracyclines upon treatment of 10μM for 2h in MelJuSo cells and histone eviction capacity of these drugs indicated by EC_{50} (time in which 50% of the histonen are evicted). Ordinary one-way ANOVA with multiple comparisons, ** p< 0.01, *** p< 0.001, **** p< 0.0001. **B** Schematic representation of the screening outline. MelJuSo melanoma cells were transduced with the Brunello genome-wide CRISPR knockout library, and cells were either or not treated with aclarubicin (100nM) for 9 days followed by gRNA sequencing. **C** Genes for which at least two different gRNAs were enriched (> 2.5-fold) in both aclarubicin-treated samples and which were significantly enriched based on RSA analysis. **D** MelJuSo cells transduced with the indicated CRISPR constructs were analyzed for p53-expression using Western blot.

Fig. 1 continued – **E** MelJuSo cells as in **C** were treated with HMD201 for 3 days and viability was assessed and normalized to untreated cells. N=3 independent experiments. Ordinary one-way ANOVA with multiple comparisons, **** p< 0.0001. **F** Indicated MelJuSo cells were treated for 2h with various concentrations of aclarubicin after which the drug was washed out and cells were left to grow for another 3 days before assessing cell viability. N=3 independent experiments. IC_{50} for each cell line is indicated. Two-tailed t-test, ** p< 0.01. **G** Colony formation assay for indicated MelJuSo cells. Cells were treated for 2h with aclarubicin, after which the drug was washed out and cells were left to grow out for 6-9 days before fixation and staining with Crystal Violet. **H** Quantification of four independent colony formation experiments, signal was normalized to the respective untreated cells. Ordinary two-way ANOVA with multiple comparisons, * p< 0.05, ** p< 0.01.

P53 is a major determinant in cellular sensitivity to aclarubicin

To test whether the function of p53 is conserved in multiple cell lines, we used the same approach to deplete p53 from 93.05 melanoma cells. In both long-term and short-term growth assays, p53-deficient cells were more resistant to aclarubicin (Fig. 2A and B and Fig. S2A). Similarly, p53-deficient MEL202 uveal melanoma and HCT116 colon lines were less sensitive to aclarubicin (Fig. 2C). To identify whether p53-status is a critical determinant for the sensitivity of cells to aclarubicin, we tested a panel of 16 different p53-wt and p53-mutant cell lines. Interestingly, based on the IC_{50}-values, the two groups almost completely segregated, arguing that the sensitivity of cells to aclarubicin can quite accurately be predicted based on p53-mutational status (Fig. 2D). This dependence on p53 activity suggests that aclarubicin might synergize with p53-stabilizing drugs. To test this, MelJuSo cells were incubated with low-dose of HDM201 (p53-MDM2 inhibitor) in the presence of different doses of aclarubicin. While aclarubicin single treatment already decreased cell viability, the combination treatment was even more effective, indicating that p53 stabilization by HDM201 acts synergistically with aclarubicin-induced chromatin damage activity (Fig. 2E). A similar observation was made for MEL202 cells, where co-treatment of the MDM2 antagonist RG7112 synergized with various concentrations of aclarubicin (Fig. 2F). These data indicate that p53 status is a major determinant for sensitivity towards the anthracycline drug aclarubicin.

Aclarubicin stabilizes and activates p53

The fact that aclarubicin induces histone eviction together with the involvement of p53 in cellular sensitivity suggests that p53 can sense the inflicted chromatin damage and subsequently translates this into a downstream signal. P53-activating signals, such as DNA damage, lead to p53 phosphorylation and stabilization, after which p53 induces the expression of target genes involved in cell cycle arrest and cell death.[16] To study the function of p53 upon induction of chromatin damage, we tested whether p53 levels were affected by aclarubicin exposure. Already after 2h of treatment, p53 stabilization and enhanced p53-S15 phosphorylation was observed by Western blot

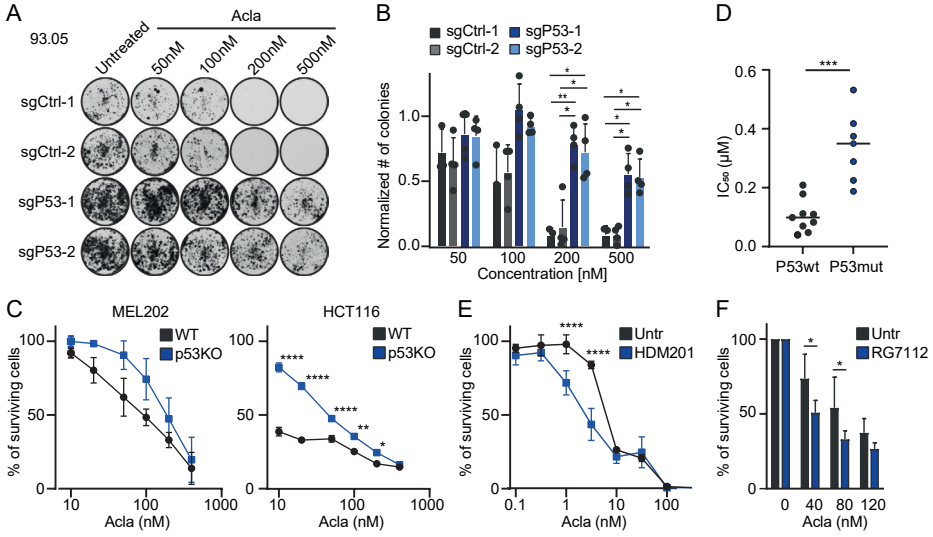

Fig. 2 p53 is a major determinant in the sensitivity of cells to aclarubicin. A Colony forming assay for 93.05 melanoma cells transduced with the indicated CRISPR constructs. Cells were treated with aclarubicin for 2h, washed and 7-9 days later fixed and stained with Crystal Violet. **B** Quantification of three independent experiments, signal was normalized to the respective untreated cells. Ordinary two-way ANOVA with multiple comparisons, * p< 0.05, ** p< 0.01. **C** Mel202 and HCT116 control cells or p53KO were treated with aclarubicin for 2h, washed, and 3 days later viability was assessed. Mel202 data represent a biological replicate, HCT116 data represent a technical triplicate. Ordinary two-way ANOVA with multiple comparisons, * p< 0.05, ** p< 0.01, **** p< 0.0001. **D** From 16 cell lines from different tissues (9 p53 WT and 7 p53 mutant) the IC_{50} was determined by exposing cells to aclarubicin for 2h and measuring viability three days later. IC_{50} represent the average of three independent experiments, and cell lines were clustered based on p53 status. Two-tailed t-test, *** p< 0.001. **E** MelJuSo cells were treated with the indicated concentrations of aclarubicin for 2h, drug was washed out, and 500nM HDM201 was added when indicated. Three days later, viability was measured and normalized to the untreated control either or not treated with HDM201. Data represent four independent experiments, Ordinary two-way ANOVA with multiple comparisons **** p< 0.0001. **F** MEL202 cells were treated for 2h with the indicated concentrations of aclarubicin, drug was washed away and cells were left to grow out in the presence or absence of 250nM RG7112. Three days later, cell viability was measured and normalized to the non-aclarubicin treated controls. Data represent three (120nM) or four (40 and 80nM) independent experiments. Statistical significance was determined by a Student's t-test * p< 0.05.

(Fig. 3A). In addition, aclarubicin treatment resulted in a p53-dependent increased expression of p53-target genes such as p21 (Fig. 3A, 3B), MDM2 and PUMA (Fig. 3B). For other genotoxic triggers, ATM kinase is activated by phosphorylation, subsequently inducing p53 phosphorylation.[17] ATM was also phosphorylated following aclarubicin

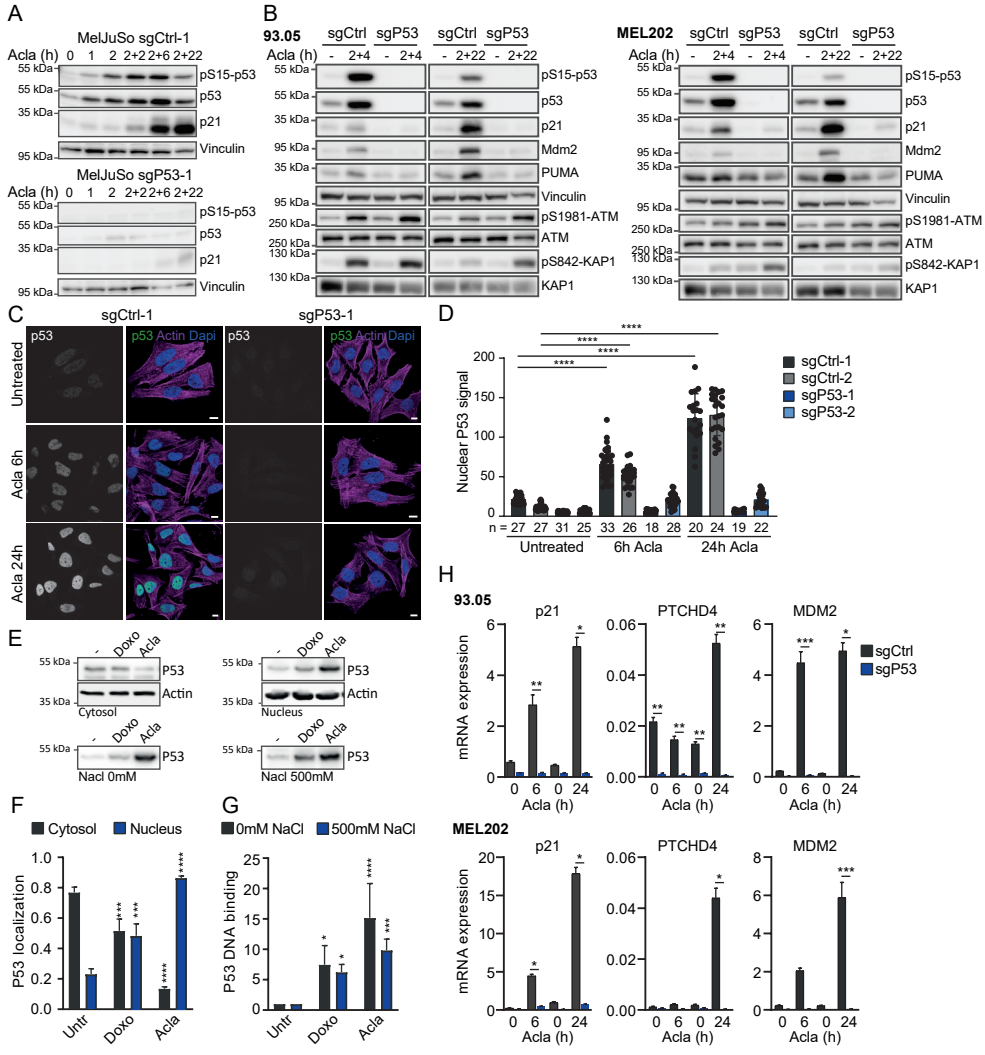

Fig. 3 Aclarubicin induces phosphorylation and activation of p53. A MelJuSo cells were exposed to 200nM aclarubicin for the indicated time points and washed away after maximum 2h, after which cells were left to recover for the indicated time points before lysis and analysis by Western blot. **B** 93.05 and MEL202 melanoma cells were exposed to aclarubicin for 2h, washed and lysed 4h or 22h later, before analysis of the indicated proteins by Western blot. **C** Representative confocal image of fixed MelJuSo cells stained for endogenous p53. Cells were treated with 200nM aclarubicin for 2h, washed and fixed at the indicated time points post treatment. DAPI and actin are stained as nuclear and cytosolic marker, respectively. Scale bar; 10µm. **D** Quantification of endogenous p53 levels. N = number of cells analyzed per condition. Ordinary two-way ANOVA with multiple comparison, **** $p < 0.0001$. **E** Chromatin binding assay for endogenous p53 in MelJuSo cells. Cells were treated with 10µM doxo- or aclarubicin for 45 minutes followed by fractionation. P53 localization and DNA binding was analyzed by Western Blot. **F** Quantification of cytosolic and nuclear p53 localization.

Fig. 3 continued – Ordinary two-way ANOVA with multiple comparisons *** p< 0.001, **** p< 0.0001. **G** Quantification of DNA binding. Ordinary two-way ANOVA with multiple comparisons * p< 0.05, *** p< 0.001, **** p < 0.0001. **H** 93.05 and MEL202 cells were exposed for 2h to 200nM aclarubicin and RNA was isolated 4h (6h) or 22h (24h) post treatment. Expression of indicated mRNA was detected using qRT-PCR and normalized to housekeeping gene expression.

N=2 independent experiments, data represent technical triplicates. Statistical significance was determined by a Student's t-test, * p<0.05, ** p< 0.01, *** p< 0.001.

treatment, as well as KAP1, another ATM substrate, suggesting that the histone evicting anthracycline aclarubicin likewise activates ATM and the subsequent stress response (Fig. 3B). Furthermore, nuclear stabilization for endogenous p53 by aclarubicin treatment was observed by microscopy (Fig. 3C and D and Fig. S3A).

To confirm that enhanced nuclear p53 also associated with DNA to drive transcription, we analyzed DNA-binding of p53 using a chromatin-association assay. Indeed, p53 was found to accumulate in the nucleus upon treatment with aclarubicin (doxorubicin was used as a positive control[18], while at the same time cytosolic p53 levels were diminished (Fig. 3E and F). Furthermore, aclarubicin treatment resulted in more p53 binding to DNA (Fig. 3E and G). To verify that aclarubicin treatment activates p53, subsequently leading to DNA binding and transcription of its target genes, we performed qRT-PCR experiments for different p53-target genes. Expression of several p53-target genes were drastically increased by aclarubicin, whereas expression of these genes was unaltered in p53-null cells upon aclarubicin treatment (Fig. 3H, S3B and S3C). Taken together, these data indicates that anthracycline variants that only have histone eviction activity, such as aclarubicin also activate p53 for increased expression of its target genes.

Aclarubicin activates p53 to induce apoptosis

p53 induces the expression of several pro-apoptotic genes[16], suggesting aclarubicin-induced p53 activation inflicts cell death via apoptosis. In line with this, several pro-apoptotic factors such as PUMA, DR4 and DR5 were upregulated by aclarubicin-treatment (Fig. 3B, 4A), whereas the anti-apoptotic factor survivin was downregulated (Fig. S4). Most of this effect was governed by p53, since it was absent in the p53-null cells. However, for some factors, such as the pro-apoptotic factors BIM and BMF, increased expression was also observed in the p53-deficient cells (Fig. 4A). Furthermore, direct apoptosis induction by aclarubicin was measured using a Caspase-GLO assays. In all three melanoma cell lines tested, a robust increase in caspase activation after aclarubicin was observed, which was largely absent in cells deficient for p53 (Fig. 4B). Similar results were obtained when detecting the cleavage of caspase substrate PARP by Western blot (Fig. 4C and D).

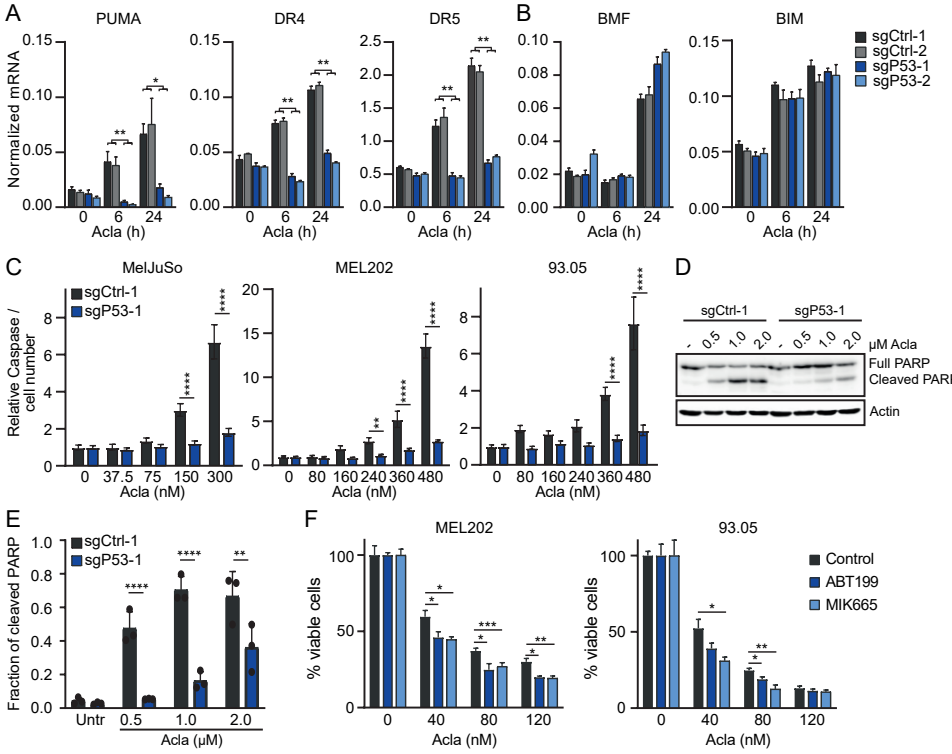

Fig. 4 Aclarubicin induces p53-dependent apoptosis. A-B Indicated MelJuSo cells were treated with 200nM aclarubicin for 2h and RNA was isolated 4h (6h) or 22h (24h) post treatment. Expression of indicated mRNA was detected using qRT-PCR and normalized to housekeeping gene expression. N=2 independent experiments, data represent technical triplicates. Statistical significance was determined by a Student's t-test, * p<0.05, ** p< 0.01. **C** Indicated cells were exposed to different concentrations of aclarubicin for 2h. Three days later cell viability and Caspase-Glo signal was detected. Caspase-Glo signal was normalized to the cell count. N=2 independent experiments, data represent technical triplicates. Two-way ANOVA with multiple comparisons, ** p< 0.01, **** p< 0.0001. **D** Indicated MelJuSo cells were exposed to different concentrations of aclarubicin for 2h, 24h post treatment cells were collected. PARP cleavage was analyzed by Western blot. Position of PARP and its cleaved form is indicated. Actin was used as a loading control. **E** Quantification of the fraction of cleaved PARP. Two-way ANOVA with multiple comparisons, ** p< 0.01, **** p< 0.0001. **F** Indicated cell lines were treated for 2h with different concentrations of aclarubicin, drug was washed away and cells were left to grow out in the presence or absence of 200nM MIK665 or 4uM ABT-199. Three days later, cell viability was measured and normalized to the non-aclarubicin treated controls. Data represent three independent experiments. Student's t-test * p< 0.05, ** p< 0.01, *** p< 0.001.

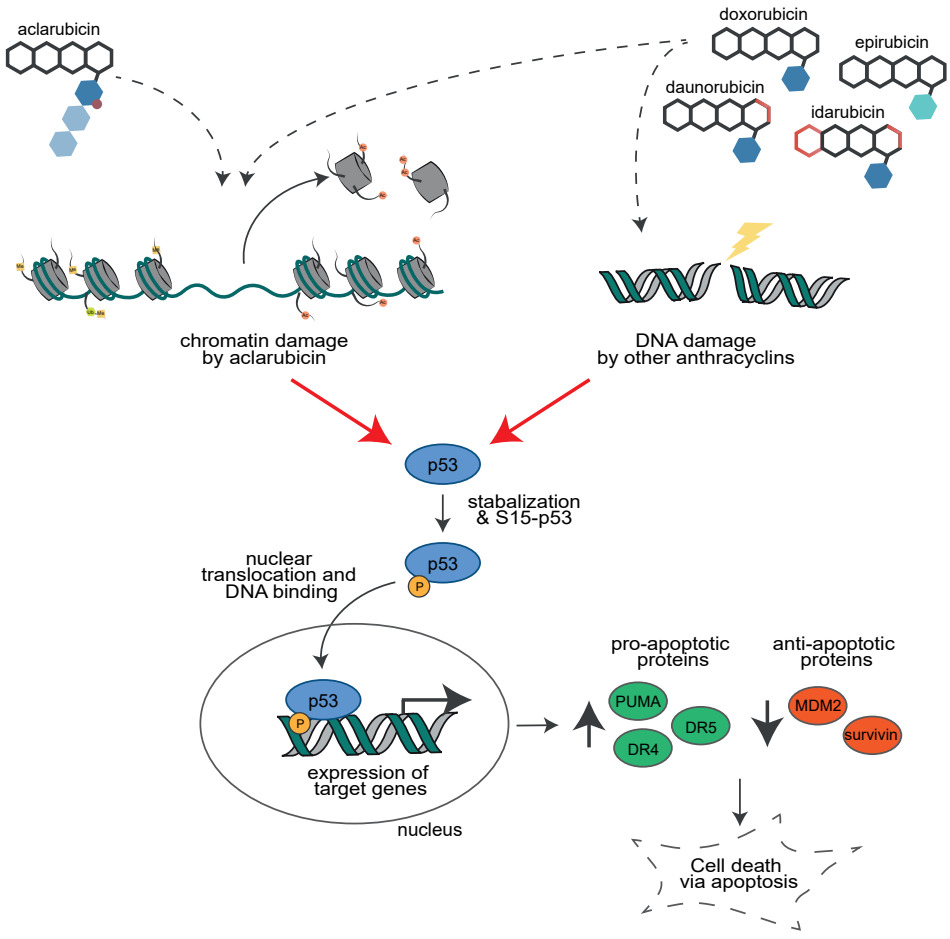

Fig. 5 Model of p53 mediated apoptosis upon anthracycline treatment. Topoisomerase II poisons like doxo-, dauno-, epi- and idarubicin introduce DNA damage via the formation of topoisomerase-DNA complexes. These drug-mediated DNA breaks subsequently leads to p53 activation. The histone evicting anthracycline aclarubicin can also inflicts p53 relocalization and activation of downstream signaling. Clinical anthracycline drugs (with both DNA- and chromatin damage) thus activate p53 dependent apoptosis by two different mechanism.

Several activators of apoptosis have been developed, such as inhibitors of the anti-apoptotic factors BCL-2 (ABT-199, also known as venetoclax) and MCL-1 (MIK665).[19] We tested whether these inhibitors synergize with aclarubicin treatment to increase cell toxicity. When using sublethal concentrations of either ABT-199 or MIK665, aclarubicin synergized with these inhibitors to tip the balance and induce cell death in all three melanoma cell lines (Fig. 4D, 4E). Thus, aclarubicin treatment leads to activation of p53, which then induces cell death via activation of the apoptosis pathway (Fig. 5).

Discussion

Aclarubicin has been considered a distinct member of the anthracycline family due to its inability to poison Topoisomerase II and inflict DNA double strand breaks. We and others have recently shown that its ability to evict histones is critical to its anti-cancer activity. But, how this activity translates to cell death has remained unclear. Using CRISPR-screening, we identified and established a key role for p53 in this process, where cellular sensitivity can be predicted fairly well solely based on p53-status. Furthermore, we showed that aclarubicin activates a p53-dependent transcriptional program inducing cell cycle arrest and apoptosis similar to DNA damaging compounds. Thus, even in the absence of DNA breaks, chromatin damage as caused by aclarubicin treatment can activate p53 and induce cell death. Thus, regular topoisomerase II-poisoning anthracyclines have two pathways initiating p53 activation for apoptosis; one initiated by the DNA damage response (as is the case for DNA damage inducing variant such as doxorubicin and daunorubicin) and the other one initiated by the chromatin damage response as visualized through the response to aclarubicin. Whether p53 itself can sense aclarubicin-induced chromatin damage or how p53 gets mobilized upon aclarubicin treatment remains to be elucidated. Possibly ATM plays a role in this, since we observe ATM activation shortly after aclarubicin treatment. In addition, in the absence of p53, apoptosis is still observed, but at greatly reduced efficiency. This implies that multiple chromatin damage sensing mechanisms might be in play.

Our data that chromatin damage activates p53 and induces apoptosis are in line with reports about other chromatin damaging agents such as the curaxins.[20,21] Curaxins can trap the FACT-complex on DNA, leading to activation of casein kinase 2(CK2) and thereby phosphorylation of p53 at Ser392. Aclarubicin treatment also induces FACT binding to DNA[21], suggesting that the aclarubicin- induced phosphorylation at p53 residue Ser392 we observe is likely mediated by FACT and CK2. However, this is likely not the sole mechanism of p53 activation. Where only p53 phosphorylation at Ser392 is observed for chromatin damage induced by curaxins[20,22], we identified additional swift induction of the DNA damage marker p53-Ser15 upon treatment with aclarubicin. This specific modification on p53 is likely induced by ATM, since we observe ATM activation determined by phosphorylation on residue Ser1981. The existence of multiple chromatin damage sensing mechanisms would also explain why we failed to identify any proteins of this pathway in the CRISPR screen. Upon p53 activation, several downstream signaling cascades are activated, leading to apoptosis. Whilst we observe p53-dependent apoptosis, and cell death is increased upon addition of apoptosis-activators, other forms of cell death are induced by aclarubicin as well, because blocking apoptosis using apoptosis inhibitor Z-VAD-FMK did not render cells significantly more resistant to aclarubicin (Fig. S5). Thus,

while p53-dependent apoptosis might be the dominant mechanism, in its absence cells will succumb via alternative pathways.

Aclarubicin is used for the treatment of acute myeloid leukemia (AML), as part of the CAG regimen (cytarabine, aclarubicin and G-CSF), both as first line treatment and for relapsed cases.[14,23,24] Our data suggest that p53-mutations would be a good stratification method for aclarubicin-treatment to identify which patients would benefit and simultaneously prevent that patients receive ineffective treatment. While p53 is mutated in only about 5-10% of the de novo AML cases, it is more frequently observed in therapy-related AML (25-33%).[25–28] In both cases, loss of p53 is strongly correlated with poor outcome and prognosis. Unfortunately, these patients will probably benefit less from an aclarubicin-based treatment, and other treatments have to be developed surpassing the prerequisite for p53. Alternatively, aclarubicin could still be effective in inducing cell death of p53-deficient cells, but then requires higher concentrations. This could be a basis for 'high-dose chemotherapy'. As aclarubicin lacks many treatment limiting side effects[7,14], using it at a higher dose can be considered. The stratification of the p53 status of AML and other tumors may be a reason to aim for normal or high-dose chemotherapies in the treatment of cancer patients. Recently, the BCL-2 inhibitor venetoclax (ABT-199) was approved as frontline treatment for AML, which is particularly useful for patients that are unable to tolerate classical intense chemotherapy, including older patients (>75 years old). Our data shows that aclarubicin synergizes with ABT-199 to increase cell toxicity, indicating that p53 wild-type AML patients would benefit from the combination therapy, with limited toxicity due to low adverse effects of both drugs.

In conclusion, we identified p53 as a major determinant in cellular sensitivity towards the anthracycline drug aclarubicin. While aclarubicin does not induce DNA double strand breaks, like other anthracycline family members, the chromatin damage induced by this drugs inflicts p53 relocalization and activation, resulting in p53 dependent apoptosis.

Materials and methods

Reagents

Aclarubicin (sc-200160) was purchased from Santa Cruz Biotechnology (USA) and dissolved in dimethylsulfoxide at 5mg/ml concentration, aliquoted and stored at -20°C for further use. Doxorubicin was obtained from Pharmachemie (the Netherlands). HDM201 and RG7112 were obtained from (Selleckchem), Venetoclax/ABT-199 (Tocris), MIK665 (MedChemExpress).

Cell culture

MelJuSo cells were cultured in IMDM supplemented with 8% fetal calf serum and cell line authentication was performed by Eurofins Genomics (19-ZE-000487). HEK293T cells (obtained from ATCC (CRL-3216)) and the cutaneous melanoma cell line 93.05 , a gift from Sjoerd van den Burg en Els Verdegaal (LUMC, Leiden, The Netherlands), were cultured in DMEM supplemented with 8% fetal calf serum. MEL202 cells were grown in mixture RPMI/DMEM-F12 + 10% FCS. The MEL202 cell line was provided by Dr. Bruce Ksander, Dept. Ophthalmology, Harvard University, Boston, USA. The generation of monoclonal p53-KO derivatives of 93.05 and MEL202 cells has been described.[29] HCT116-Ctrl and p53KO cells were a gift from Bert Vogelstein and grown in DMEM/10% FCS.[30] p53-wildtype (A549, FM3, HeLa, MelJuSo, U2OS, U87) and p53-mutant (BT474, BXPC3, DU145, K562, PC3, SKBR3 and U118) cells were cultured and tested as described before.[10] All cell lines were maintained in a humidified atmosphere of 5% CO_2 at 37°C and regularly tested for the absence of mycoplasma.

CRISPR-activation and knockout screen

For knockout screening, the human CRISPR Brunello genome-wide knockout library was a gift from David Root and John Doench (Addgene #73178). Two batches of $1x10^8$ MelJuSo melanoma cells were infected at an MOI of 0.3. Transduced cells were selected using puromycin (1µg/ml) for five days. After the selection procedure, cells were treated continuously with aclarubicin at a concentration of 100nM for 9 days. After this, cells were grown out for an additional 3 days and genomic DNA was isolated from the aclarubicin-treated cells, as well as from the control population that was grown in parallel. gDNAs were amplified using the established protocol.[31] gRNAs were sequenced using the Illumina NovaSeq6000 and inserts were mapped to the reference. Statistical analysis was done using RSA analysis, enrichment >2.5 was considered a candidate hit.[32]

Transductions

For the generation of viral particles, HEK293T cells were transfected using polyethyleneimine (Polyscience Inc.) with packaging plasmids pRSVrev, pHCMV-G VSV-G and pMDLg/pRRE in combination with the lentiviral construct. Virus was harvested, filtered and target cells were transduced in the presence of 8µg/ml polybrene (Millipore).

Hit validation and subcloning

For validation of the knockout screen, two individual guides per gene were cloned into the LentiCRISPR v2 vector (a gift from Feng Zhang, Addgene plasmid #52961) and the indicated cells were transduced and selected using puromycin. Guide sequences were as follows: p53-1: 5'-CCATTGTTCAATATCGTCCG-3', p53-2: 5'- GGTGCCCTATGAGCCGCCTG-3'. For genomic validation, genomic DNA was isolated and a PCR fragment of ±300bp was cloned into an emptied GFP-C1 vector (clonetech) using NEBBuilder HiFi fidelity assembly mix using the

following primers: p53-1-fw: ATATCTGGAGTTCCGCATATGGGTAAGGACAAGGGTTGGGC, p53-1-rv: CGCTCTAGATCCGGTGGATCCGGAAGGGACAGAAGATGACAGGG, p53-2-fw: ATATCTGGAGTTCCGCATATGGTCCCCAGGCCTCTGATTC, p53-2-rv: CGCTCTAGATCCGGTGGATCCGAGGCCCTTAGCCTCTGTAAGC. Sequences were verified using Ori Fw: GGAGCCTATGGAAAAACGCC and Ori rv: TTAACGCTTACAATTTACGCG.

Long-term proliferation assays

Cells were seeded into 12-well plates (5000 cells/well). The next day, drugs were added at concentrations indicated and incubated for 2 hours. Subsequently, cells were washed extensively and left to grow for 7 to 9 days. For fixing and staining, cells were washed with PBS and incubated for 20 min at RT with Crystal violet staining solution (0.05% w/v Crystal Violet, 1% formaldehyde, 1% methanol in 1X PBS). Quantification of colonies was done by extraction of the crystal violet. To do so, colonies were incubated for 20 min. at RT with 15% acetic acid (500µL). Read out was done by measuring the absorbance using a CLARIOstar plate reader (BMG Labtech).

Short-term growth assays

Cells were seeded into 96-well plates and exposed the next day with indicated drugs and concentrations. When indicated, drugs were removed two hours later and cells were cultured for an additional 72 hours. Cell viability was measured using the CellTiter-Blue viability assay (Promega). Relative survival was normalized to the untreated control and corrected for background signal.

Apoptosis assay

Cells were seeded in triplicate in white-walled 96-well plates with clear bottoms and in clear 96-well plates. The next day, the cells were exposed to indicated compound(s). Three days later, caspase 3 /7 activity was assessed with the use of the Caspase-Glo 3/7 Assay (Promega), and cell viability was assessed with the CellTiter-Blue Cell Viability Assay. Relative caspase activity was normalized to cell number.

Chromatin association assay

Cells were seeded into 6cm dishes (1x10^6 cells/well). The next day, indicated drugs were added for 30 min. at 10µM final concentration. Cells were lysed in lysis buffer (25mM HEPES pH 7.6, 5mM $MgCl_2$, 25mM KCl, 0.05mM EDTA, 10% glycerol, 0.1% NP-40) for 30 minutes at 4°C and nuclei were spun down and resuspended in 75µL buffer (20mM Tris-HCl pH 7.6, 3mM EDTA). Of this, 25µL samples were adjusted to the indicated NaCl concentrations to a total volume of 50µL and incubated for 20 min. on ice. Subsequently, chromatin was spun down and resuspended in SDS-sample buffer (2% SDS, 10% glycerol, 5% β-mercaptoethanol, 60 mM Tris-HCl pH 6.8 and 0.01% bromophenol blue) after which samples were analyzed by SDS-PAGE and Western blotting.

Western blot

Upon treatment as indicated, cells were washed extensively to remove drugs. Cells were collected and lysed directly in SDS-sample buffer (2% SDS, 10% glycerol, 5% β-mercaptoethanol, 60 mM Tris-HCl pH 6.8 and 0.01% bromophenol blue). Lysates were resolved by SDS/PAGE followed by Western blotting. Primary antibodies used for blotting: P53 (DO-1, sc-126 Santa Cruz), γH2AX (1:1000, 05-036, Millipore), β-actin (A5441, Sigma), pS15p-53 (#9284, Cell Signaling Technology), pS1981-ATM (Clone 10H11.E12; Rockland Immunochemicals), ATM (Clone Y170; Merck Millipore), pS842-KAP1 (A300-767A; Bethyl Laboratories), KAP1 (A300-274A; Bethyl Laboratoris), Mdm2 (Clone 3G9; Merck Millipore), PUMA (Clone G3; Santa Cruz Biotechnology), p21 (clone CP74; Merck Millipore), PARP (#9542, Cell Signaling Technology), Vinculin (clone hVIN-1; Sigma-Aldrich). Images were quantified with ImageJ.

Microscopy

For endogenous p53 staining cells were seeded on coverslips, and the next day exposed for the indicated time with 200nM aclarubicin. Upon treatment, cells were fixed in 4% formaldehyde, permeabilized with 0.1% Triton, blocked in 0.5% BSA and stained with mouse monoclonal anti-P53 (DO1, sc-126, Santa Cruz), goat-anti-mouse-Alexa-Fluor-488 (Thermo fisher Scientific), Alexa-Fluor-647-phalloidin (A22287, Thermo fisher Scientific) and DAPI. Cells were analyzed by a Leica SP8 confocal microscope system with 63x lens. Cells stably expressing PAGFP-H2A were used for histone eviction experiments. Photoactivation and time-lapse confocal imaging were performed as described [6] and loss of fluorescence from the photoactivated region after different treatments was quantified. Quantification was done using ImageJ software.

RT-PCR

RNA was isolated using the SV total RNA isolation kit (Promega), after which cDNA was synthesized using the reverse transcriptase reaction mixture as indicated by Promega. qPCR was performed using SYBR green mix (Roche Diagnostics, Indianapolis, IN, USA) in a C1000 touch Thermal Cycler (Bio-Rad laboratories, Hercules, CA, USA). In independent experiments the expression of target genes was determined and normalized to at least two housekeeping genes *CAPNS1* and *SRPR*. Primers for detection:

Primer name	Sequence Forward	Sequence Reverse
BIM/BCL2L11	5′-CATCGCGGTATTCGGTTC	5′-GCTTTGCCATTTGGTCTTTTT
BMF	5′-TTTATGGCAATGCTGGCTATCG	5′-GCAATCTGTACCTCTGCTTGATG
CAPNS1	5′-ATGGTTTTGGCATTGACACATG	5′-GCTTGCCTGTGGTGTCGC
CDKN1A/p21	5′-AGCAGAGGAAGACCATGTGGA	5′-AATCTGTCATGCTGGTCTGCC
DR4/TNFRSF10A	5′-CTACCTCCATGGGACAGCAC	5′-TGCAGCTGAGCTAGGTACGA
DR5/TNFRSF10B	5′-AAGACCCTTGTGCTCGTTGT	5′-AGGTGGACACAATCCCTCTG
MDM2	5′-ACGCACGCCACTTTTTCTCT	5′-TCCGAAGCTGGAATCTGTGAG
NOXA	5′ ACTGTTCGTGTTCAGCTC	5′- AGCACACTCGACTTCC
PTCHD4	5′- TATTTTGCTCCAGGCTGAGG	5′-ATGGCTCTGGCTGACTTGAC
PUMA/BBC3	5′-GACCTCAACGCACAGTA	5′- TAATTGGGCTCCATCT
SRPR	5′-CATTGCTTTTGCACGTAACCAA	5′-ATTGTCTTGCATGCGGCC
Survivin	5′-AAAGCATTCGTCCGGTTG	5′-TCCGCAGTTTCCTCAAATTC

Data and statistical analysis

For in vitro experiment, each sample was assayed in biological triplicate, unless stated otherwise. No statistical methods were used to predetermine sample size. All error bars denote mean + SD. Statistical analysis were performed using Prism 8 software (Graphpad Inc.) or Microsoft excel. Western blot and confocal data were quantified using ImageJ software. Significance is represented on the graphs as follow: ns, not significant, *$p < 0.05$, **$p < 0.01$, ***$p < 0.001$, ****$p < 0.0001$.

Acknowledgements

This work was supported by the Institute for Chemical Immunology, an NWO Gravitation project funded by the Ministry of Education, Culture and Science of the Netherlands and a Spinoza award both to J.N. We thank J.J Akkermans for help with the genomic validation of the MelJuSo P53 KO lines.

References

(1) Hortobágyi, G. N. Anthracyclines in the Treatment of Cancer. An Overview. *Drugs*. **1997**, *54 Suppl 4*, 1–7.

(2) Martins-Teixeira, M. B.; Carvalho, I. Antitumour Anthracyclines: Progress and Perspectives. *ChemMedChem*. **2020**, *15*, 933–948.

(3) Nitiss, J. L. Targeting DNA Topoisomerase II in Cancer Chemotherapy. *Nature Reviews Cancer 2009 9:5*. **2009**, *9*, 338–350.

(4) van der Zanden, S. Y.; Qiao, X.; Neefjes, J. New Insights into the Activities and Toxicities of the Old Anticancer Drug Doxorubicin. *The FEBS Journal*. **2021**, *288*, 6095–6111.

(5) Perego, P.; Corna, E.; De Cesare, M.; Gatti, L.; Polizzi, D.; Pratesi, G.; Supino, R.; Zunino, F. Role of Apoptosis and Apoptosis-Related Genes in Cellular Response and Antitumor Efficacy of Anthracyclines. *Current medicinal chemistry*. **2001**, *8*, 31–37.

(6) Pang, B.; Qiao, X.; Janssen, L.; Velds, A.; Groothuis, T.; Kerkhoven, R.; Nieuwland, M.; Ovaa, H.; Rottenberg, S.; Van Tellingen, O.; Janssen, J.; Huijgens, P.; Zwart, W.; Neefjes, J. Drug-Induced Histone Eviction from Open Chromatin Contributes to the Chemotherapeutic Effects of Doxorubicin. *Nature Communications 2013 4:1*. **2013**, *4*, 1–13.

(7) Qiao, X.; Van Der Zanden, S. Y.; Wander, D. P. A.; Borràs, D. M.; Song, J. Y.; Li, X.; Duikeren, S. Van; Gils, N. Van; Rutten, A.; Herwaarden, T. Van; Tellingen, O. Van; Giacomelli, E.; Bellin, M.; Orlova, V.; Tertoolen, L. G. J.; Gerhardt, S.; Akkermans, J. J.; Bakker, J. M.; Zuur, C. L.; Pang, B.; Smits, A. M.; Mummery, C. L.; Smit, L.; Arens, R.; Li, J.; Overkleeft, H. S.; Neefj, J. Uncoupling DNA Damage from Chromatin Damage to Detoxify Doxorubicin. *Proceedings of the National Academy of Sciences of the United States of America*. **2020**, *117*, 15182–15192.

(8) Pang, B.; de Jong, J.; Qiao, X.; Wessels, L. F. A.; Neefjes, J. Chemical Profiling of the Genome with Anti-Cancer Drugs Defines Target Specificities. *Nature chemical biology*. **2015**, *11*, 472–480.

(9) Yang, F.; Kemp, C. J.; Henikoff, S. Anthracyclines Induce Double-Strand DNA Breaks at Active Gene Promoters. *Mutation Research/Fundamental and Molecular Mechanisms of Mutagenesis*. **2015**, *773*, 9–15.

(10) Wander, D. P. A.; Van Der Zanden, S. Y.; Van Der Marel, G. A.; Overkleeft, H. S.; Neefjes, J.; Codée, J. D. C. Doxorubicin and Aclarubicin: Shuffling Anthracycline Glycans for Improved Anticancer Agents. *Journal of Medicinal Chemistry*. **2020**, *63*, 12814–12829.

(11) Wander, D. P. A.; van der Zanden, S. Y.; Vriends, M. B. L.; van Veen, B. C.; Vlaming, J. G. C.; Bruyning, T.; Hansen, T.; van der Marel, G. A.; Overkleeft, H. S.; Neefjes, J. J. C.; Codée, J. D. C. Synthetic (N , N -Dimethyl)Doxorubicin Glycosyl Diastereomers to Dissect Modes of Action of Anthracycline Anticancer Drugs. *The Journal of Organic Chemistry*. **2021**, *86*, 5757–5770.

(12) Lotrionte, M.; Biondi-Zoccai, G.; Abbate, A.; Lanzetta, G.; D'Ascenzo, F.; Malavasi, V.; Peruzzi, M.; Frati, G.; Palazzoni, G. Review and Meta-Analysis of Incidence and Clinical Predictors of Anthracycline Cardiotoxicity. *The American journal of cardiology*. **2013**, *112*, 1980–1984.

(13) Mistry, A. R.; Felix, C. A.; Whitmarsh, R. J.; Mason, A.; Reiter, A.; Cassinat, B.; Parry, A.; Walz, C.; Wiemels, J. L.; Segal, M. R.; Adès, L.; Blair, I. A.; Osheroff, N.; Peniket, A. J.; Lafage-Pochitaloff, M.; Cross, N. C. P.; Chomienne, C.; Solomon, E.; Fenaux, P.; Grimwade, D. DNA Topoisomerase II in Therapy-Related Acute Promyelocytic Leukemia. *New England Journal of Medicine*. **2005**, *352*, 1529–1538.

(14) Qiao, X.; van der Zanden, S. Y.; Li, X.; Tan, M.; Zhang, Y.; Song, J. Y.; van Gelder, M. A.; Hamoen, F. L.; Janssen, L.; Zuur, C. L.; Pang, B.; van Tellingen, O.; Li, J.; Neefjes, J. Diversifying the

Anthracycline Class of Anti-Cancer Drugs Identifies Aclarubicin for Superior Survival of Acute Myeloid Leukemia Patients. *Molecular Cancer*. **2024**, *23*, 1–16.

(15) Yang, F.; Kemp, C. J.; Henikoff, S. Doxorubicin Enhances Nucleosome Turnover around Promoters. *Current biology : CB*. **2013**, *23*, 782–787.

(16) Lavin, M. F.; Gueven, N. The Complexity of P53 Stabilization and Activation. *Cell Death & Differentiation 2006 13:6*. **2006**, *13*, 941–950.

(17) Canman, C. E.; Lim, D. S.; Cimprich, K. A.; Taya, Y.; Tamai, K.; Sakaguchi, K.; Appella, E.; Kastan, M. B.; Siliciano, J. D. Activation of the ATM Kinase by Ionizing Radiation and Phosphorylation of P53. *Science (New York, N.Y.)*. **1998**, *281*, 1677–1679.

(18) Scala, F.; Brighenti, E.; Govoni, M.; Imbrogno, E.; Fornari, F.; Treré, D.; Montanaro, L.; Derenzini, M. Direct Relationship between the Level of P53 Stabilization Induced by RRNA Synthesis-Inhibiting Drugs and the Cell Ribosome Biogenesis Rate. *Oncogene*. **2016**, *35*, 977–989.

(19) Mukherjee, N.; Skees, J.; Todd, K. J.; West, D. A.; Lambert, K. A.; Robinson, W. A.; Amato, C. M.; Couts, K. L.; Van Gullick, R.; MacBeth, M.; Nassar, K.; Tan, A. C.; Zhai, Z.; Fujita, M.; Bagby, S. M.; Dart, C. R.; Lambert, J. R.; Norris, D. A.; Shellman, Y. G. MCL1 Inhibitors S63845/MIK665 plus Navitoclax Synergistically Kill Difficult-to-Treat Melanoma Cells. *Cell death & disease*. **2020**, *11*.

(20) Gasparian, A. V.; Burkhart, C. A.; Purmal, A. A.; Brodsky, L.; Pal, M.; Saranadasa, M.; Bosykh, D. A.; Commane, M.; Guryanova, O. A.; Pal, S.; Safina, A.; Sviridov, S.; Koman, I. E.; Veith, J.; Komar, A. A.; Gudkov, A. V.; Gurova, K. V. Curaxins: Anticancer Compounds That Simultaneously Suppress NF-KB and Activate P53 by Targeting FACT. *Science Translational Medicine*. **2011**, *3*.

(21) Nesher, E.; Safina, A.; Aljahdali, I.; Portwood, S.; Wang, E. S.; Koman, I.; Wang, J.; Gurova, K. V. Role of Chromatin Damage and Chromatin Trapping of FACT in Mediating the Anticancer Cytotoxicity of DNA-Binding Small Molecule Drugs. *Cancer research*. **2018**, *78*, 1431.

(22) Luzhin, A.; Rajan, P.; Safina, A.; Leonova, K.; Stablewski, A.; Wang, J.; Robinson, D.; Isaeva, N.; Kantidze, O.; Gurova, K. Comparison of Cell Response to Chromatin and DNA Damage. *Nucleic acids research*. **2023**, *51*, 11836–11855.

(23) Wei, G.; Ni, W.; Chiao, J. W.; Cai, Z.; Huang, H.; Liu, D. A Meta-Analysis of CAG (Cytarabine, Aclarubicin, G-CSF) Regimen for the Treatment of 1029 Patients with Acute Myeloid Leukemia and Myelodysplastic Syndrome. *Journal of hematology & oncology*. **2011**, *4*.

(24) Jin, J.; Wang, J. X.; Chen, F. F.; Wu, D. P.; Hu, J.; Zhou, J. F.; Hu, J. Da; Wang, J. M.; Li, J. Y.; Huang, X. J.; Ma, J.; Ji, C. Y.; Xu, X. P.; Yu, K.; Ren, H. Y.; Zhou, Y. H.; Tong, Y.; Lou, Y. J.; Ni, W. M.; Tong, H. Y.; Wang, H. F.; Mi, Y. C.; Du, X.; Chen, B. A.; Shen, Y.; Chen, Z.; Chen, S. J. Homoharringtonine-Based Induction Regimens for Patients with de-Novo Acute Myeloid Leukaemia: A Multicentre, Open-Label, Randomised, Controlled Phase 3 Trial. *The Lancet. Oncology*. **2013**, *14*, 599–608.

(25) Daver, N. G.; Iqbal, S.; Huang, J.; Renard, C.; Lin, J.; Pan, Y.; Williamson, M.; Ramsingh, G. Clinical Characteristics and Overall Survival among Acute Myeloid Leukemia Patients with TP53 Gene Mutation or Chromosome 17p Deletion. *American journal of hematology*. **2023**, *98*, 1176–1184.

(26) Papaemmanuil, E.; Gerstung, M.; Bullinger, L.; Gaidzik, V. I.; Paschka, P.; Roberts, N. D.; Potter, N. E.; Heuser, M.; Thol, F.; Bolli, N.; Gundem, G.; Van Loo, P.; Martincorena, I.; Ganly, P.; Mudie, L.; McLaren, S.; O'Meara, S.; Raine, K.; Jones, D. R.; Teague, J. W.; Butler, A. P.; Greaves, M. F.; Ganser, A.; Döhner, K.; Schlenk, R. F.; Döhner, H.; Campbell, P. J. Genomic Classification and Prognosis in Acute Myeloid Leukemia. *The New England journal of medicine*. **2016**, *374*, 2209–2221.

(27) George, B.; Kantarjian, H.; Baran, N.; Krocker, J. D.; Rios, A. TP53 in Acute Myeloid Leukemia: Molecular Aspects and Patterns of Mutation. *International journal of molecular sciences*. **2021**, *22*.

(28) Wong, T. N.; Ramsingh, G.; Young, A. L.; Miller, C. A.; Touma, W.; Welch, J. S.; Lamprecht, T. L.; Shen, D.; Hundal, J.; Fulton, R. S.; Heath, S.; Baty, J. D.; Klco, J. M.; Ding, L.; Mardis, E. R.; Westervelt, P.; Dipersio, J. F.; Walter, M. J.; Graubert, T. A.; Ley, T. J.; Druley, T. E.; Link, D. C.; Wilson, R. K. Role of TP53 Mutations in the Origin and Evolution of Therapy-Related Acute Myeloid Leukaemia. *Nature*. **2015**, *518*, 552–555.

(29) Heijkants, R. C.; Teunisse, A. F. A. S.; de Jong, D.; Glinkina, K.; Mei, H.; Kielbasa, S. M.; Szuhai, K.; Jochemsen, A. G. MDMX Regulates Transcriptional Activity of P53 and FOXO Proteins to Stimulate Proliferation of Melanoma Cells. *Cancers*. **2022**, *14*, 4482.

(30) Bunz, F.; Dutriaux, A.; Lengauer, C.; Waldman, T.; Zhou, S.; Brown, J. P.; Sedivy, J. M.; Kinzler, K. W.; Vogelstein, B. Requirement for P53 and P21 to Sustain G2 Arrest after DNA Damage. *Science (New York, N.Y.)*. **1998**, *282*, 1497–1501.

(31) Joung, J.; Konermann, S.; Gootenberg, J. S.; Abudayyeh, O. O.; Platt, R. J.; Brigham, M. D.; Sanjana, N. E.; Zhang, F. Genome-Scale CRISPR-Cas9 Knockout and Transcriptional Activation Screening. *Nature Protocols 2017 12:4*. **2017**, *12*, 828–863.

(32) König, R.; Chiang, C. Y.; Tu, B. P.; Yan, S. F.; DeJesus, P. D.; Romero, A.; Bergauer, T.; Orth, A.; Krueger, U.; Zhou, Y.; Chanda, S. K. A Probability-Based Approach for the Analysis of Large-Scale RNAi Screens. *Nature methods*. **2007**, *4*, 847–849.

Supporting information chapter 3

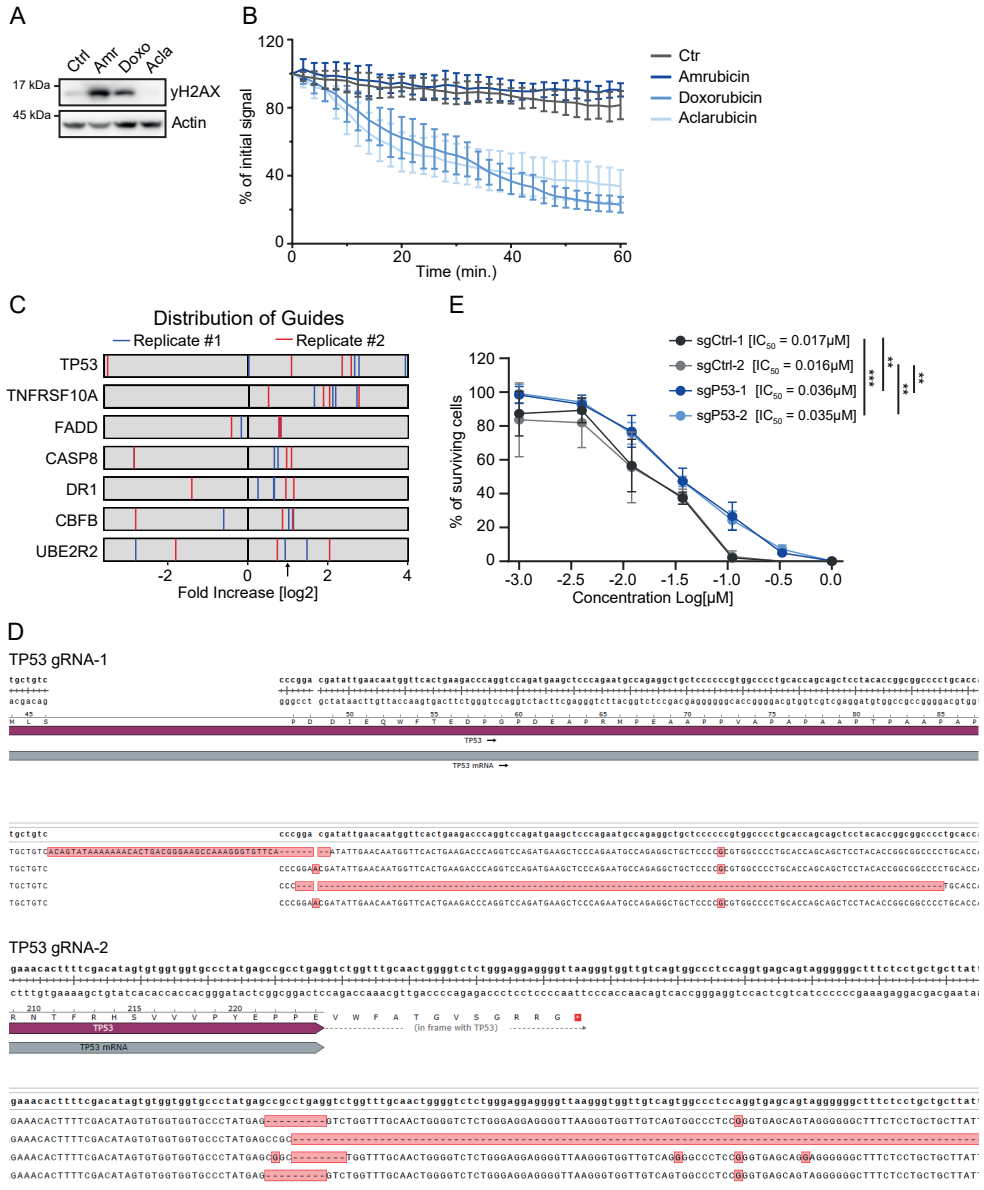

Fig. S1 p53 as a regulator of sensitivity to aclarubicin. A Western blot showing DNA double strand breaks induced by three different anthracycline drugs in MelJuSo cells treated for 2hr with 10uM. Actin was used as a loading control. Corresponding to quantification in Fig. 1A, bottom panel. **B** Fluorescent signal of photo activated GFP-H2A histones was followed in living cells over time upon treatment with the different drugs. Quantification of loss of initial signal upon histone eviction is plotted. Corresponding to quantification of EC_{50} in Fig. 1A, bottom panel.

Fig S1. Continued – **C** gRNA enrichment for hits with at least two guides per sort enriched >2.5-fold. Arrow depicts 2.5-fold threshold and red and blue stripes represent enrichment of individual gRNAs compared to the non-sorted population. **D** Snapshot of Snapgene, showing genomic validation of pooled MelJuSo P53-knock out cell lines. **E** Indicated MelJuSo cells were treated for 72h with various concentrations of aclarubicin followed by assessing the cell viability. N=3 independent experiments. IC_{50} for each cell line is indicated. Two-tailed t-test, ** p< 0.01, *** p< 0.001.

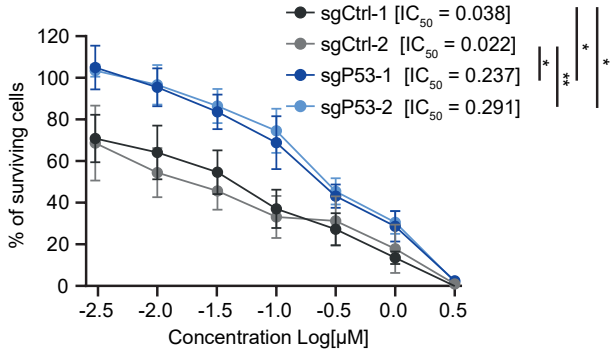

Fig. S2 p53 as a major determinant in sensitivity to Aclarubicin. Indicated 93.05 cells were treated for 2h with various concentrations of aclarubicin after which the drug was washed out and cells were left to grow for another 3 days before assessing cell viability. N=3 independent experiments. IC_{50} for each cell line is indicated. Two-tailed t-test, * p< 0.05, ** p< 0.01.

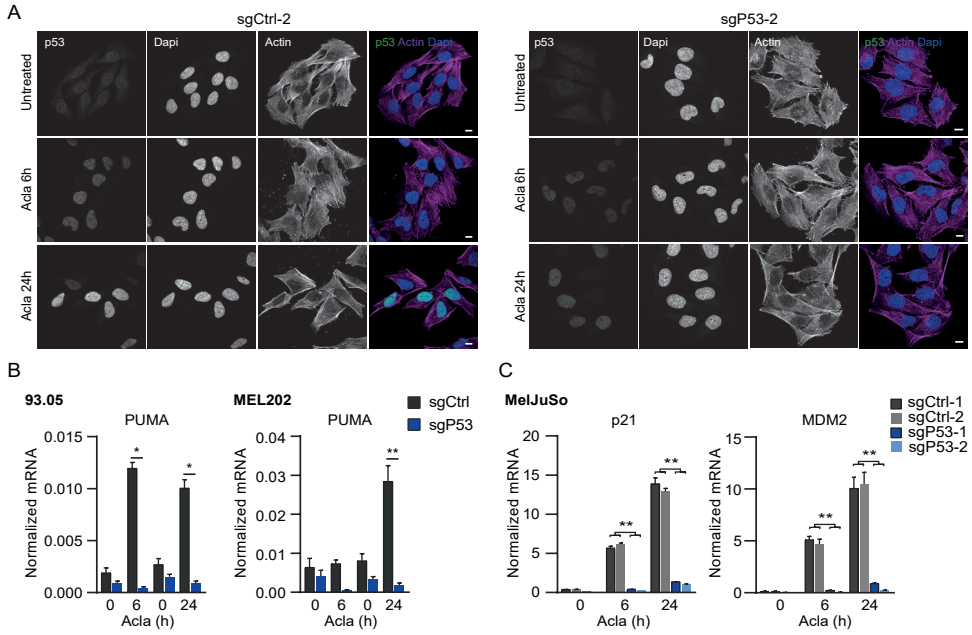

Fig. S3 Aclarubicin induces nuclear accumulation and activation of p53. A Representative confocal images of fixed MelJuSo cells stained for endogenous p53. Cells were treated with 200nM aclarubicin for 2h, washed and fixed at the indicated time points post treatment. DAPI and actin are stained as nuclear and cytosolic marker, respectively. Scale bar; 10µm. **B** 93.05 and MEL202 cells were exposed for 2h to 200nM aclarubicin and RNA was isolated 4h (6h) or 22h (24h) post treatment. Expression of indicated mRNA was detected using qRT-PCR and normalized to housekeeping gene expression. N=2 independent experiments, data represent technical triplicates. Statistical significance was measured using a Student's t-test, * $p<0.05$, ** $p< 0.01$. **C** Indicated MelJuSo cells were exposed for 2h to 200nM aclarubicin and RNA was isolated 4h (6h) or 22h (24h) post treatment. Expression of indicated mRNA was detected using qRT-PCR and normalized to housekeeping gene expression. N=2 independent experiments, data represent technical triplicates. Statistical significance was determined by a Student's t-test, ** $p< 0.01$.

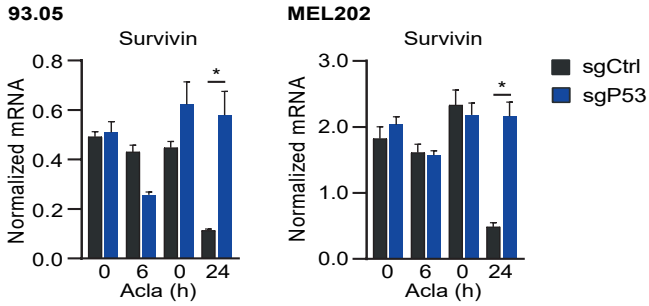

Fig. S4 Aclarubicin induces p53-dependent decrease of survivin expression. Indicated cells were treated with 200nM aclarubicin for 2h and RNA was isolated 4h (6h) or 22h (24h) post treatment. Expression of indicated mRNA was detected using qRT-PCR and normalized to housekeeping gene expression. N=2 independent experiments, data represent technical triplicates. Statistical significance was determined by a Student's t-test, * p<0.05.

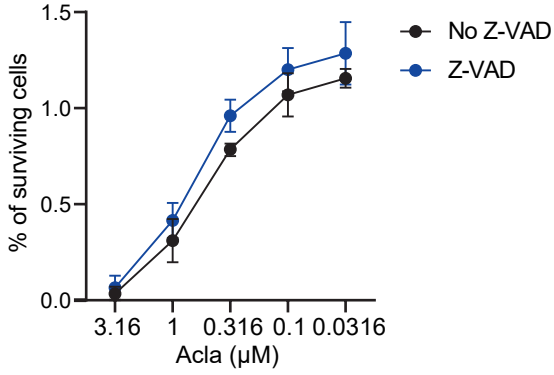

Fig. S5 Z-VAD did not render cells significantly more resistant to aclarubicin. MelJuSo cells were treated for 2h with different concentrations of aclarubicin, drug was washed away and cells were left to grow out in the presence or absence of Z-VAD-FMK. Three days later, cell viability was measured and normalized to the non-aclarubicin treated controls. Data represent two independent experiments. Statistical significance was determined by a wo-way ANOVA with multiple comparisons, data is ns.